ELEVENTH EUROPEAN ROTORCRAFT FORUM

Paper No.68

AEROELASTIC STABILITY OF ROTOR BLADES BY LIFTING SURFACE THEORY AND FINITE ELEMENT METHOD

Fu Changqing and Wang Shicun

Aircraft Department
Nanjing Aeronautical Institute
Nanjing, China

September 10—13, 1985
London, England

THE CITY UNIVERSITY, LONDON, ECIV OHB, ENGLAND

AEROELASTIC STABILITY OF ROTOR BLADES BY LIFTING SURFACE THEORY AND FINITE ELEMENT METHOD

Fu Changqing and Wang Shicun
Aircraft Department
Nanjing Aeronautical Institute, China

Abstract

The finite element formulation based on the principle of minimum potential energy for the spatial discretization of the equations of motion governing rotor blade aeroelastic problems is presented. A numerical lifting surface method based on the velocity potential is used to evaluate the unsteady airloads on a hovering rotor in compressible flow. The blade is divided into a number of equally spaced elements. Instead of the Hermite polynomials in helicopter dynamics new polynomials are used to define the shape functions so as to reduce both the computer storage and time required. The equations of motion are linearized assuming blade motion to be a small perturbation about the steady deflected shape. The flutter equations of motion are solved in an iterative modification of the conventional V-g method. The formulation is applied to hingeless helicopter rotor blades. Numerical results show sensitivity of the aeroelastic stability boundaries to the unsteady airloads.

Introduction

The fundamental problem in helicopter aeroelasticity is the coupled flap-lag-torsion aeroelastic problem of a rotor blade involving nonlinear structural, inertial, and aerodynamic forces[1],[2]. A comprehensive set of equations of motion of blades has been presented[3]. These equations were developed from nonlinear strain displacement relations, using both Hamilton's principle and the Newtonian method.

A better approach for discretizing helicopter rotor blade aeroelastic equations is based on the finite element method, which enables one to discretize the partial differential equations of motion directly. Consequently, a significant reduction in the algebraic manipulative labor required for solving the problem, in comparison with the methods of solution based on the modal method, is accomplished. The finite element method is very flexible and the formulation can be easily

adapted to different rotor blade configurations. Nonuniformities in blade properties can be easily accommodated. In Ref. 4-7 the bending degrees of freedom are discretized by using a conventional beam type bending element based on Hermite polynomials, i.e. cubic interpolation for bending.

The helicopter rotor is subject to unsteady flow phenomena in its operation. Various unsteady aerodynamic strip theories have been developed for rotary wing applications[9] [10]. Friedmann and Yuan[11]have applied the modified unsteady aerodynamic strip theory to the rotor blade aeroelastic problems in hovering flight when all three (flap, lag, and torsion) degrees of freedom are considered.

Two-dimensional strip theory does not allow for curvature and finite aspect ratio effects of helicopter rotor blades. Jones and Moore[12]have developed a simple numerical lifting surface technique for calculating the aerodynamic coefficients on oscillating wings in subsonic flight. Rao and Jones[13] have applied this simple but general method of predicting airloads to helicopter rotor blades on a full three-dimensional basis. Ref. 14 has also treated the similar problem using isoparametric finite element method. The method takes finite aspect ratio and subsonic compressibility effects into account. With a realistic wake representation, Rao and Schatzle[15] have developed a numerical lifting surface method to predict the unsteady airloads on a hovering rotor blade in compressible flow.

In the present paper, the finite element method is used to study the flutter stability of coupled flap-lag-torsion of a rotor blade in hover. The blade is divided into a number of equally spaced elements. Each end of the blade has an additional virtual element. Every element consists of two nodes with four degrees of freedom at each node. These degrees of freedom represent elastic displacements in the axial, lead-lag, flap directions and elastic twist about elastic axis, respectively. The new polynomials[8] are used to represent the bending and the torsional degrees of freedom. In comparision with the usual shape function based on Hermite polynomials, the main features of the present method are of higher accuracy and more economy in computing storage and time requirements. The element forces are obtained by applying the principle of minimum potential energy and the assembly of the elements yields the equations of motion in terms of the nodal degrees of freedom.

The lifting surface theory for the unsteady compressible flow developed in the past for rotary wing aeroelastic analyses is modified in the paper so as to make it applicable to the coupled flap-lag-torsion

aeroelastic problem of a rotor blade in hover. These corrections are primarily due to variable lead-lag velocity, constant angle of attack and constant inflow[11]. Isoparametric finite element method is used to determine the distribution of the doublet strengths on the blade. Once the appropriate distribution of the doublet strengths has been found, it is relatively easy to determine the aerodynamic loads per unit span acting on the rotor blade.

The nonlinear equations of motion are solved for steady state blade deflections through an iterative procedure. The equations of motion are linearized assuming blade motion to be a small perturbation about the steady deflected shape. The flutter equations of motion are solved in an iterative modification of the conventional V-g method. The formulation is applied to hingeless helicopter rotor blades. Numerical results show sensitivity of the aeroelastic stability boundaries to the unsteady airloads.

This is the first attempt to determine the flutter stability boundaries of a coupled flap-lag-torsion rotor blade using the lifting surface theory based on the velocity potential and the finite element method based on the principle of minimum potential energy, with the new shape functions, directly.

The Principle of Minimum Potential Energy

The rotor blade is treated as an elastic beam rotating with constant angular velocity Ω. The rectangular coordinate system x, y, z is attached to the undeformed blade which is at a precone angle of β_P. The origin is at the root of the blade, the x axis coincides with the elastic axis, and the y axis is in the plane of rotating pointed towards the leading edge (Fig.1).

A few important assumptions made in the derivation of the equations of motion are: (1). The blade is assumed to have moderate deflections, i.e. small strains and finite slopes. (2). There is no coupling between blade and fuselage dynamics. (3). The simple numerical lifting surface technique is used to calculate the aerodynamic loads on the rotor blade; compressibility is considered, but stall is neglected.

Blade bending deformations shown in Fig. 1 are described by the displacements of the elastic axis u,v,w in the x,y,z directions respectively. A point on the elastic axis that is located at (x, 0, 0) in the x, y, z coordinate system before deformation is located at $x+u$, v, w after deformation. Then the blade cross section undergoes a rotation θ_1 about the deformed elastic axis.

The equations of motion are obtained using the principle of minimum potential energy:

$$\delta\Pi = \delta U - \delta W = 0 \tag{1}$$

where

$$\delta U = \int_0^R (\delta U_S + \delta U_I) dx \tag{2}$$

$$\delta W = \int_0^R (L_u \delta u + L_v \delta v + L_w \delta w + M_\phi \delta\phi) dx \tag{3}$$

where U_S and U_I are respectively strain energy and inertial potential energy, W is the work done due to nonconservative external forces, L_u, L_v, L_w and M_ϕ are the external loads distributed along the length of the blade in the axial, lag, flap and torsion directions respectively.

The expressions for the variation of the strain energy and the inertial loading can be found in Ref. 3.

$$\delta U_I = \int_0^R -[P_x \delta u + P_y \delta v + P_z \delta w + q_z \delta v' - q_y \delta w' + (q_x + v' q_y + w' q_z)\delta\phi] dx \tag{4}$$

The energy expressions δU_S, δU_I, δW can be nondimensionalized by dividing them by $m_0 \Omega^2 R^3$, where m_0 is a reference mass per unit length. The nondimensional deflections v/R, w/R, ϕ are assumed to be of order ε, where ε is a small nondimensional parameter such that $\varepsilon^2 \ll 1$. The other nondimensional quantities and their assumed orders of magnitude can be found in Ref.5. The lowest order terms in δU and δW are of order ε^2. Terms of order ε^4 and higher are neglected. Some linear third-order terms, which are important for the torsion equation, are kept.

Finite Element Discretizaton

The first step in solving the equations of motion is the discretization of the spatial dependence. The blade is divided into a number of beam elements with equal length. Each end of the blade has a virtual element. Every element consists of two nodes (Fig.2) with four degrees of freedom namely u, v, w, ϕ at each node.

The principle of minimum potential energy, Eq.(1), is discretized as

$$\delta\Pi = \sum_{i=1}^{n} \delta\Pi_i = 0 \tag{5}$$

with

$$\delta \Pi_i = \delta U_i - \delta W_i \tag{6}$$

where δU_i and δW_i are respectively the potential energy and work contribution of the ith element and n is total number of elements. The distributions of the deflections u, v, w and ϕ over an element are represented in terms of polynomials. Nodal degrees of freedom are written as

$$\begin{Bmatrix} u \\ v \\ w \\ \phi \end{Bmatrix} = [N]\{q_i\} \tag{7}$$

where the shape function matrix $[N]$ is

$$[N] = \begin{bmatrix} N_1 N_2 N_3 N_4 & 0 & 0 & 0 & 0 & 0 & 0 & 0 & 0 & 0 & 0 & 0 \\ 0 & 0 & 0 & 0 & N_1 N_2 N_3 N_4 & 0 & 0 & 0 & 0 & 0 & 0 & 0 \\ 0 & 0 & 0 & 0 & 0 & 0 & 0 & 0 & N_1 N_2 N_3 N_4 & 0 & 0 & 0 \\ 0 & 0 & 0 & 0 & 0 & 0 & 0 & 0 & 0 & 0 & 0 & 0 \end{bmatrix} \begin{matrix} \\ \\ \\ N_1 N_2 N_3 N_4 \end{matrix} \tag{8}$$

and the vector of element degree of freedom $\{q_i\}$ is defined as

$$\{q_i\} = [u_{i-2}\, u_{i-1}\, u_i\, u_{i+1}\, v_{i\ 2}\, v_{i\ 1}\, v_i\, v_{i+1}\, w_{i-2}\, w_{i-1}\, w_i\, w_{i+1}\, \phi_{i\ 2}\, \phi_{i-1}\, \phi_i\, \phi_{i+1}]^T \tag{9}$$

The shape functions in Eq.(8) are defined as

$$\begin{aligned} N_1 &= -\frac{1}{2h^3} x_i^3 + \frac{1}{h^2} x_i^2 - \frac{1}{2h} x_i \\ N_2 &= \frac{3}{2h^3} x_i^3 - \frac{5}{2h^2} x_i^2 + 1 \\ N_3 &= -\frac{3}{2h^3} x_i^3 + \frac{2}{h^2} x_i^2 + \frac{1}{2h} x_i \\ N_4 &= \frac{1}{2h^3} x_i^3 - \frac{1}{2h^2} x_i^2 \end{aligned} \tag{10}$$

where h is the length of the element, $h = R/n$, and x_i is the local axial coordinate for the ith element, measured from the left end of the element.

For single load path blades, for example, hingeless and articulated blades, the axial displacement u can be eliminated in terms of the other deflections v, w, and ϕ and the centrifugal force. Nodal degrees of freedom are obtained by dropping all terms associated with u from Eq.(7).

Formulation of Aerodynamic Loads

The aerodynamic loads in hover, distributed along the length of the blade, are obtained using Jones-Moore aerodynamic lifting surface theory.

It differs from most other methods in that it is based on the use of the velocity rather than the acceleration potential of the flow. The velocity potential satisfies the wave equation. It can be shown that the soluton of the wave equation may be derived from the singular integral equation.

The space variables x, y, z are replaced by $\tilde{x}$, $\tilde{y}$, $\tilde{z}$, respectively, so that

$$\tilde{x}=\sqrt{1-M^2}\,\frac{x}{R},\quad \tilde{y}=\frac{y}{R},\quad \tilde{z}=\sqrt{1-M^2}\,\frac{z}{R} \tag{11}$$

From Green's theorem a relation between the downwash velocity at a point on a wing and a distribution of doublets over the wing and wake surfaces is

$$4\pi\tilde{W}=\iint K\frac{\partial^2}{\partial\tilde{z}^2}\left(\frac{e^{-ikr}}{r}\right)dS \tag{12}$$

where $\tilde{W}$ is the transformed downwash; K, the local doublet intensity, is equal to the discontinuity in the transformed potential across the wing or wake; r is the distance from a field point to collocation point in transformed coordinates; S is surface area in transformed coordinats.

The vertical displacement ζ of the blade is assumed to have a steady-state component ζ_s due to coning and constant angle of attack, as well as an unsteady component due to flapping and twisting about this steady position, i.e.

$$\zeta=\zeta_s+\zeta_f e^{i\omega t}+\zeta_t e^{i\omega t} \tag{13}$$

where

$$\begin{aligned}\zeta_s&=x\beta_P+y\theta_0\\ \zeta_f&=f(x)Z_{tP}\\ \zeta_t&=F(x)\alpha_{tP}\end{aligned} \tag{14}$$

where $f(x)$ and $F(x)$ are the flapping mode and torsional mode relative to tip, respectively. The downwash is

$$\tilde{W}=\frac{\partial\zeta}{\partial t}+V_0\frac{\partial\zeta}{\partial y} \tag{15}$$

$$\tilde{W}=\tilde{W}_s+\tilde{W}_f+\tilde{W}_t \tag{16}$$

where subscripts s, f, t represent steady-state condition, flapping motion and torsional motion, respectively. The solutions for steady flow and unsteady flow are obtained by using Eqs.(14), (15) and (12).

The helical wake of the rotor blade is assumed to extend rearwards as indicated in Fig.3. Any distortion of the wake due to blade-tip vortex

interference is ignored. The rotor blade is divided into a number of isoparametric elements on which the distribution of the doublet strengths is assumed to be polynomial. Extending from each trailing edge panel is a wake strip. From Ref. [14] once the appropriate doublet strength distribution has been found, it is then relatively easy to determine the aerodynamic forces per unit span acting on the rotor blade.

Jones-Moore theory[12],[13] is not directly applicable to rotor blades undergoing coupled flap-lag-torsion motion. The approximate modifications, similar to Ref.11, are introduced here. The expressions of lift and moment about the elastic axis of the blade can be written as

$$L=\frac{1}{2}\rho V_0^2 c[L_0\theta_0+(L_1+iL_2)\frac{2\Delta h}{c}+(L_3+iL_4)\Delta\alpha]+\frac{1}{8}a\rho c^2\Delta\dot{V}\theta_0+$$
$$+\frac{a}{2\sqrt{1-M^2}}\rho V_0 c\theta_0\Delta V[1+c(K)]-\frac{a}{2\sqrt{1-M^2}}\rho V c U_{b0} \qquad (17)$$

$$M_\phi=\frac{4}{1}\rho V_0^2 c^2[M_0\theta_0+(M_1+iM_2)\frac{2\Delta h}{c}+(M_3+iM_4)\Delta\alpha]-$$
$$-\frac{1}{16}\rho a\Delta\dot{V}\theta_0 c^3\bar{a}+\frac{a}{4\sqrt{1-M^2}}\rho V_0 c^2\theta_0(\bar{a}+0.5)\Delta V[1+c(K)]-$$
$$-\frac{a}{4\sqrt{1-M^2}}\rho V c^2(\bar{a}+0.5)U_{b0} \qquad (18)$$

where L_0, M_0 are the steady airload coefficients, L_1, L_3, M_1, M_3 and L_2, L_4, M_2, M_4 are the in phase and out of phase airload coefficients, respectively. c(K) is Theodorsen lift deficiency function. $V=V_0+\Delta V$.

It is of importance to identify correctly the relationship between the variables used in unsteady aerodynamic theory and the variables used in describing the motion of the rotor blade having flap, lead-lag and torsion degrees of freedom. Fig.4 shows the blade coordinate systems and positions of the cross-section before and after the deformation. The flutter motion of the rotor blade is assumed to be a small perturbation about the trim state. The stability equations are linearized about a static equilibrium position. The velocity components of a point on the elastic axis of the blade can be written as

$$U_b=-U_{z2}=w'v\Omega+\dot{w}+v_i=U_{b0}+\Delta U_b$$
$$U_t=-U_{y2}=\dot{v}+\Omega x=U_{t0}+\Delta U_t \qquad (19)$$

The most common approach in helicopter analyses has been to identify $\Delta\dot{h}$ as the normal velocity $-\Delta U_b$ at the rotor blade and $\Delta\alpha$ as the $\Delta\phi$. For the rotor blade the quantity Δh is meaningless.

In addition to the distributed lift and torsional moment an expression

for the aerodynamic load in the chordwise direction is also required for rotor blade aeroelastic applications. This expression can be obtained by using the approximate method given in Ref.11, thus

$$L_{y2}=-L(U_b/U_t)-\frac{1}{2}C_{d0}\rho cU_t^2 \tag{20}$$

where C_{d0} is profile-drag coefficient.

From Eq.(5), the global matrices are obtained by the assembly of the element matrices. The equations of motion are

$$[M]\{\ddot{q}\}+[C]\{\dot{q}\}+[K]\{q\}+([\bar{A}(q_0)]\{q_0\}+[A(q_0)]\{\Delta q\})=\{Q\} \tag{21}$$

where $[M]$, $[C]$, $[K]$ are generalized global mass, damping, stiffness matrices. These matrices are the contributions from δU. The mass and stiffness matrices are symmetric whereas the damping matrix is antisymmetric. $[\bar{A}(q_0)]$ is the steady-state generalized aerodynamic matrix, and $[A(q_0)]$ is the generalized complex aerodynamic matrix. $\{Q\}$ is the load vector.

Method of Soluton

The equations of motion are nonlinear in $\{q\}$. The steady-state equations are obtained by dropping all time dependent terms from Eqs. (21). The displacement $\{q\}$ is written as the sum of a steady component $\{q_0\}$ and an unsteady perturbation $\{\Delta q\}$.

$$\{q\}=\{q_0\}+\{\Delta q\} \tag{22}$$

Substituting Eq.(22) into Eqs.(21), the nonlinear steady state equations are

$$([K(q_0)]+[\bar{A}(q_0)])\{q_0\}=\{Q\} \tag{23}$$

The numerical solution of the nonlinear steady state equations (23) is evaluated iteratively.

The flutter equations of motion are linearized about the steady-state position. They are

$$[M(q_0)]\{\Delta\ddot{q}\}+[C(q_0)]\{\Delta\dot{q}\}+([K(q_0)]+[A(q_0)])\cdot\{\Delta q\}=\{0\} \tag{24}$$

The mass, damping, stiffness and complex aerodynamic matrices are functions of the steady deflection $\{q_0\}$.

The normal mode method is used to solve the linearized flutter equations. Eqs. (24) are transformed to the modal space by writing

$$\{\Delta q\}=[\Phi]\{P\} \tag{25}$$

where $[\Phi]$ is the matrix of the first N eigenvectors and $\{P\}$ is the vector of N generalized coordinates in the modal space. The resulting modal-space equations are

$$[M^*]\{\ddot{P}\}+[C^*]\{\dot{P}\}+([\varpi_i^2 M_i]+[A^*])\{P\}=\{0\} \tag{26}$$

where $[M^*]$, $[C^*]$, and $[A^*]$ matices are of order N. The elements of $[M^*]$ and $[C^*]$ are in general real while $[A^*]$ has complex elements.

Eqs. (26) can be solved in an iterative modification of the conventional V-g method[11]. First an artificial damping coefficient denoted by g is introduced and combined with the flutter frequency ϖ to yield a

$$Z=\frac{1}{\varpi^2}(1+ig) \tag{27}$$

In the usual manner at the flutter condition simple harmonic motion is stipulated by assuming

$$\{P\}=\{\bar{p}\}e^{i\omega t} \tag{28}$$

Combination of Eqs. (26) through (28) yields the complex eigenvalue form

$$([D]-Z[I])\{P\}=0 \tag{29}$$

The solution to the complex eigenvalue problem given by Eq. (29) yields a number of complex eigenvalues.

Results and Discussion

The numerical results obtained are for a hingeless rotor blade with uniform spanwise properties. In the computations the following numerical values were used:

$a=6$; $C_{d0}=0.0095$; $K_{m1}/R=0$; $K_{m2}/R=0.025$

$K_A/K_m=1.5$; $C/R=\pi/40$; $\beta_P=0$; $\sigma=0.1$

$\gamma=5$; $EI_y/m_0\Omega^2R^4=0.014486$; $K_h=1.15$

$GJ/m_0\Omega^2R^4=0.000925,\ 0.005661$

Mach number M is evaluated at the blade spanwise station $0.8R$. The main purpose of this paper is to examine the sensitvity of the coupled flap-lag-torsion aeroelastic stability boundaries of a single blade in hover to the unsteady aerodynamic derivatives. The stiffnesses EI_y, GJ and the inertial parameters K_{m1}, K_{m2}, K_A are chosen such that the rotating frequencies corresponding to given values. The rotating flap frequency of the blade is taken to be $1.15\,\Omega$. Two different torsional frequencies

are considered, a frequency of $2.5\,\Omega$ represents a torsionally-soft blade and $5\,\Omega$ a torsionally-stiff blade. However the lead-lag frequency is varied over a reasonably wide range $0.5<\bar{\omega}_\zeta<2.5$ representing a relative wide range of possible blade configurations.

The convergence properties of the method are considered first. This is accomplished by changing the number of elements or the number of mode shapes in the modal reduction process. The convergence of the steady state deflections using different numbers of finite elements is presented. Fig.5 gives the accuracy of steady tip deflections v_{0tip}, w_{0tip} (nondimensionalized with respect to the rotor radius) and ϕ_{0tip} (in rad) as the total number of finite elements is varied from 2 to 6. The results show, for the case considered, that five elements are sufficient for good convergence. For comparison, the results for the steady tip geometric twist ϕ_{0tip}, when using the linear interpolation torsion element, are also shown. The performance of the latter element is inferior when compared to the torsion element based on the new interpolation which is used in this paper.

Fig.6 presents the convergence of rotating coupled natural frequencies of the soft-inplane blade about its steady deflected position as the number of finite elements is varied. It is seen that five elements are sufficient for four digit accuracy. The results obtained by using the linear interpolation torsion element are also shown, and obviously, the new interpolation is better than the linear one.

The results presented in Fig.7 show the effect of unsteady aerodynamics on the stability boundary for a torsionally-soft rotor blade. The aerodynamic center from the elastic axis is considered to be zero. As indicated in the figure the unsteady aerodynamic effect is considerable. It is evident that using the quasisteady assumption as is commonly done in rotary wing aeroelasticity tends to make the blade appear less stable than it could be in reality, however it obviously represents a conservative assumption for the cases considered.

The effect of aerodynamic center elastic axis offset on stability boundary is important. The torsionally-stiff blade with $\bar{e}_d=0$ is quite stable, and an offset $\bar{e}_d=-0.15$ between the aerodynamic center and the elastic axis reduces considerably the values of θ_c at which instability can occur. The effect of unsteady aerodynamics on the stability boundary for a torsionally-stiff blade with $\bar{e}_d=-0.15$ is illustrated by Fig.8. The unsteady aerodynamic effect considerably influences the stability boundary. This is due to the fact that the flutter frequency is high and

therefore it is sensitive to unsteady aerodynamics.

Fig.9 illustrates the effect of Mach number on the stability boundary. As shown the stability boundary is less sensitive to compressibility.

Conclusions

The finite element method based on the principle of minimum potential energy has been applied successfully to determine the aeroelastic stability of a flap-lag-torsion blade. The rotor blade is discretized into beam elements of eight nodal degrees of freedom. The new polynomials are used to define the shape functions in order to reduce both the storage space and computation time required with the same accuracy as Hermite polynomials. A velocity potential lifting surface method has been used to evaluate the steady and unsteady aerodynamic derivatives for an arbitrary hovering rotor in compressible flow. However, the unsteady aerodynamic theory has to be modified when applying it to the coupled flap-lag-torsion aeroelastic problem of a rotor blade. These modifications are primarily due to constant angle of attack, constant inflow and the lead-lag motion. Unsteady aerodynamic effect seems to be important. Neglecting the lead-lag degree of freedom may not be valid in the aeroelastic problem of a rotor having flap, lag and torsion degrees of freedom.

References

1. Friedmann, P., "Recent Developments in Rotary-wing Aeroelasticity," Journal of Aircraft, Vol.14, No.11, November 1977.
2. Friedmann, P., "Formulation and Solution of Rotary-Wing Aeroelastic stability and Response Problems," Eighth European Rotorcraft Forum, Paper No.3.2, August 1982.
3. Hodges, D.H., and Dowell, E.H., "Nonlinear Equations of Motion for the Elastic Bending and Torsion of Twisted Nonuniform Blades," NASA TN D-7818, Dec. 1974.
4. Straub, F.K., and Friedmann, P.P., "A Galerkin Type Finite Element for Rotary-Wing Aeroelasticity in Hover and Forward Flight," Sixth European Rotorcraft and Powered Lift Aircraft Forum, paper No.15, sep. 1980.
5. Sivaneri, N.T. and Chopra, I., "Dynamic Stability of a Rotor Blade Using Finite Element Analysis," Proceedings of AIAA/ASME/ASCE/AHS 22nd Structures, Structural Dynamics and Materials Conference

and AIAA Dynamics Specialist Conference, Part I, April 1981.

6. Sivaneri, N.T. and Chopra, I., "Finite Element Analysis for Bearingless Rotor Blade Aeroeelasticity," Proceedings of 38th Annual Forum of the American Helicopter Society, May 1982.
7. Fu, C.Q., "The Finite Element Method for Hingeless Helicopter Blade Flutter," M.S. Thesis, Nanjing Aeronautical Institute, 1981.
8. Cheng, G.W., "A New Interpolation Function and Some Application to Finite Element Method in Solid Mechanics," M.S. Thesis, Nanjing Aeronautical Institute, 1981.
9. Loewy, R.G., "A Two Dimensional Approximation to the Unsteady Aerodynamics of Rotary Wings," Journal of the Aeronautical Sciences, Vol.24, 1957.
10. Jones, W.P. and Rao, B.M., "Compressibility Effects on Oscillating Rotor Blades in Hovering Flight," AIAA Journal, Vol. 8, No. 2, February 1970.
11. Friedmann, P. and Yuan, C. "Effect of Modified Aerodynamic Strip Theories on Rotor Blade Aeroelastic Stability," AIAA Journal, Vol. 15, No.7, July 1977.
12. Jones, W.P. and Moore, J.A., "Simplified Aerodynamic Theory of Oscillating Thin Surfaces in Subsonic Flow," AIAA Journal, Vol. 11, No. 9, Sep. 1973.
13. Rao, B.M. and Jones, w.P., "Application to Rotary Wings of a Simplified Aerodynamic Lifting Surface Theory for Unsteady Compressible Flow," AD 775418, January 1974.
14. Fu, C, Q., "Helicopter Rotor Lifting Surface Theory for Unsteady Compressible Flow and the Solution of Finite Element Method," M. S. Thesis, Nanjing Aeronautical Institute, 1981.
15. Rao, B.M. and Schatzle, R.R., "Analysis Unsteady Airloads of Helicopter Rotors in Hover," Journal of Aircraft, Vol. 15, No. 4, 1978.

Appendix. Nomenclature

a	lift-curve slope
$\bar{a}$	offset between elastic axis and midchord, $\bar{a}=-(\bar{e}_d+0.5)$
$[A^*]$	generalized complex aerodynamic matrix
C	blade chord
C_{d0}	profile-drag coefficrent
[C]	generalized damping matrix

e_d	aerodynamic center offset from elastic axis, $\bar{e}_d = \frac{2e_d}{c}$
i	$=\sqrt{-1}$
K	doublet intensity
L	unsteady lift per unit span
L_0	steady lift per unit span
$[M]$	generalized mass matrix
M_ϕ	aerodynamic moment per unit length about elastic axis
$[N]$	shape function matrix
n	number of elements
P_x, P_y, P_z	inertial forces
$\{Q\}$	load vector
$\{q\}$	vector of global degrees of freedom
q_x, q_y, q_z	inertial moments
R	blade radius
t	time
u, v, w	elastic displacements in x, y, z directions, respectively
V	oncoming free stream velocity
V_0	constant component of V
ΔV	time dependent, harmonic part of V
x, y, z	rotating orthogonal coordinate system
x_2, y_2, z_2	orthogonal coordinate system fixed at dlade cross section
x_i	local axial coordinate of the ith element
Z	complex flutter parameter
α	blade cross-section angle of attack
β_P	blade precone angle
θ_0	constant part of pitch angle
ρ	density of air
ϕ	elastic twist about elastic axis
$\omega_v, \omega_w, \omega_\phi$	fundamental coupled rotating lead-lag, flap, torsion natural frequencies, respectively
ω	flutter frequency, $\bar{\omega} = \omega/\Omega$
Ω	rotor blade angular velocity
δ	variational notation
$(\ )'$	$\partial(\ )/\partial x$
$(*)$	$\partial(\ )/\partial t$

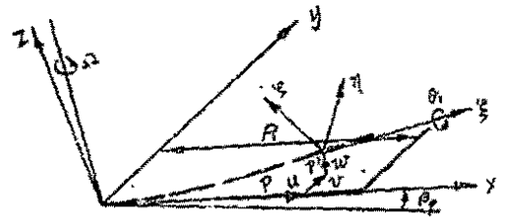

Fig.1 Blade coordinate systems

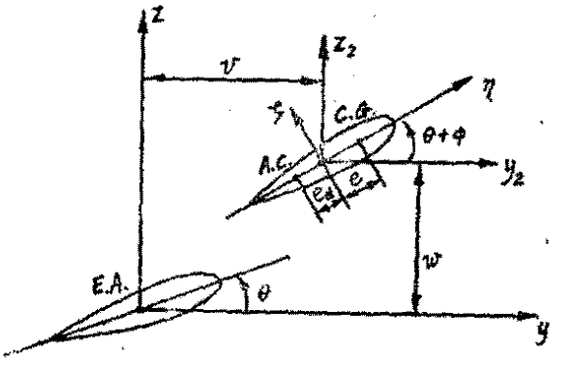

Fig.4 Positions of the cross-section before and after the deformation

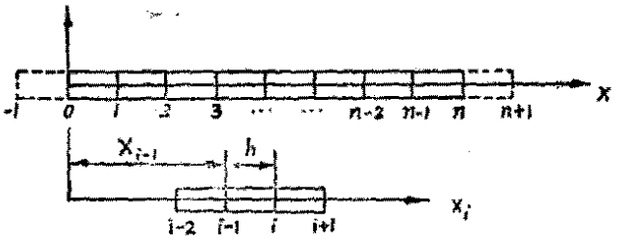

Fig.2 Rotor blade elements

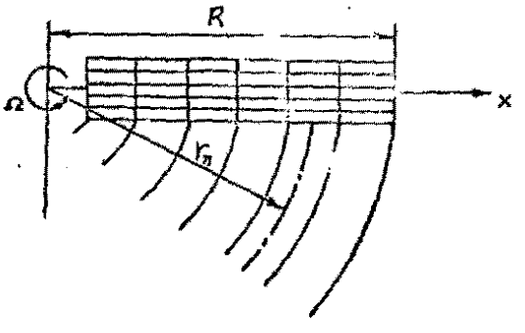

Fig.3 Schematic diagram of rotor blade and its wake

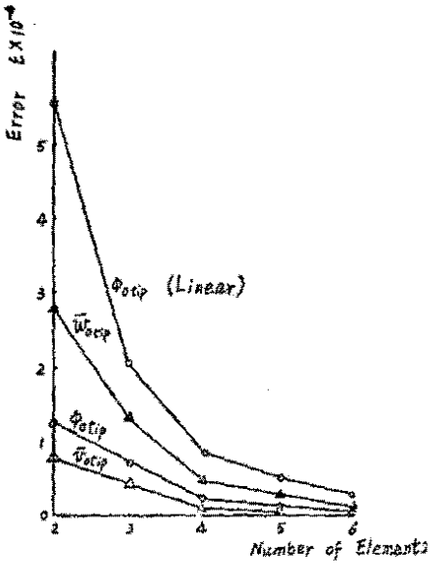

Fig.5 Accuracy of steady tip deflections of a rotor blade ($\beta_p=0$, $\bar{\omega}_v=1.5$, $\bar{\omega}_\phi=2.5$, $\theta=0.2$)

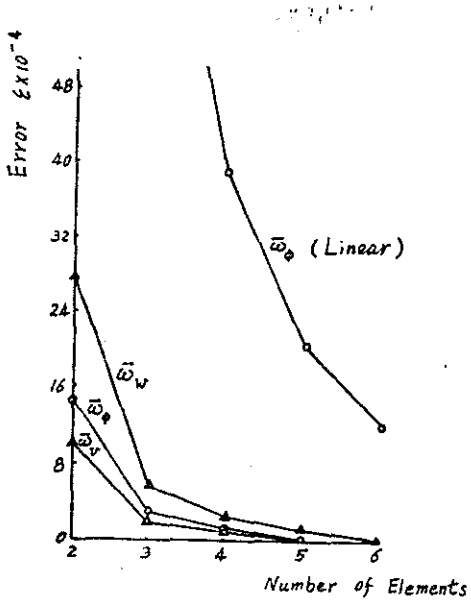

Fig.6 Accuracy of fundamental coupled natural frequencies of a rotor blade ($\beta_P = 0$, $\bar{\omega}_v = 0.7$, $\bar{\omega}_\phi = 2.5$, $\theta = 0.2$)

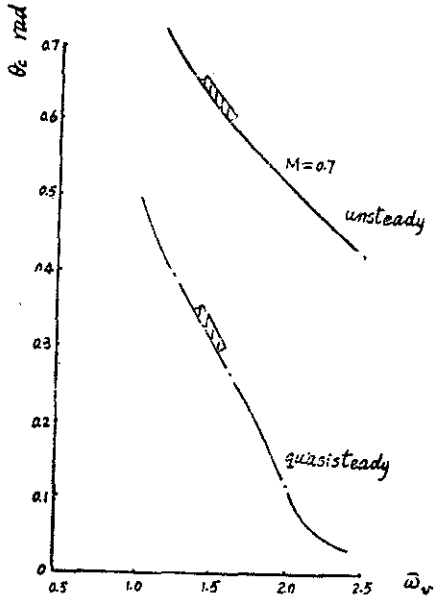

Fig.7 Effect of unsteady aerodynamics ($\beta_P = 0$, $\bar{\omega}_\phi = 2.5$, $\bar{e}_d = 0$)

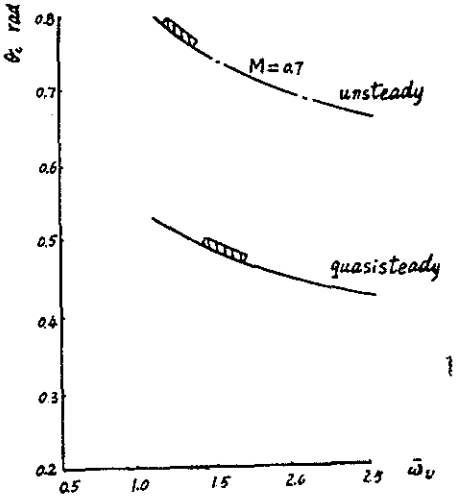

Fig.8 Effect of unsteady aerodynamics ($\beta_P = 0$, $\bar{\omega}_\phi = 5$, $\bar{e}_d = -0.15$)

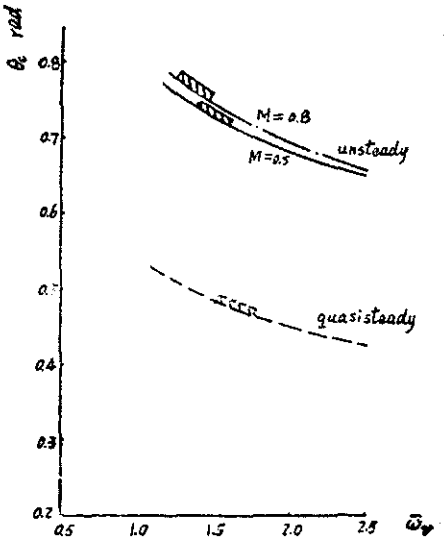

Fig.9 Effect of mach number ($\beta_P = 0$, $\bar{\omega}_\phi = 5$, $\bar{e}_d = -0.15$)